Geophysical Research Letters

RESEARCH LETTER
10.1029/2023GL105996

The Role of Passive Cloud Volumes in the Transition From Shallow to Deep Atmospheric Convection

Cristian V. Vraciu[1,2], Irene L. Kruse[3,4], and Jan O. Haerter[3,4,5,6]

[1]Department of Theoretical Physics, Horia Hulubei National Institute of Physics and Nuclear Engineering, Măgurele, Romania, [2]Faculty of Physics, University of Bucharest, Bucharest–Măgurele, Romania, [3]Leibniz Centre for Tropical Marine Research, Bremen, Germany, [4]Niels Bohr Institute, Copenhagen University, Copenhagen, Denmark, [5]Physics and Earth Sciences, Constructor University, Bremen, Germany, [6]Institute of Physics and Astronomy, University of Potsdam, Potsdam, Germany

Key Points:

- The interaction between active and passive cloud volumes (PCV) may lead to higher cloud tops
- The organization of the passive cumuli is beneficial for the transition to deep convection
- The PCV help the new updraft plumes to reach the level of free convection

Correspondence to:

C. V. Vraciu,
cristian.vraciu@theory.nipne.ro

Citation:

Vraciu, C. V., Kruse, I. L., & Haerter, J. O. (2023). The role of passive cloud volumes in the transition from shallow to deep atmospheric convection. *Geophysical Research Letters*, *50*, e2023GL105996. https://doi.org/10.1029/2023GL105996

Received 23 AUG 2023
Accepted 6 OCT 2023

Author Contributions:

Conceptualization: Cristian V. Vraciu
Formal analysis: Cristian V. Vraciu
Investigation: Cristian V. Vraciu, Irene L. Kruse
Methodology: Cristian V. Vraciu, Jan O. Haerter
Resources: Jan O. Haerter
Visualization: Cristian V. Vraciu
Writing – original draft: Cristian V. Vraciu
Writing – review & editing: Cristian V. Vraciu, Irene L. Kruse, Jan O. Haerter

Abstract Properly capturing the transition from shallow to deep convection remains a major shortcoming of numerical weather and climate models due to poor understanding of the physical processes controlling this transition. Although recent studies suggest shallow preconditioning and cold pool feedbacks to be important, these studies are unable to explain the initial phase of the transition. We identify an additional mechanism, namely the interaction between passive cloud volumes (PCV)—old cumulus cloud volumes in the decaying stage—and updrafts, and discuss the potential role of this mechanism in the transition from shallow to deep convection. We show that the number of updrafts interacting with PCV is very large during the transition and the updrafts better preserve their buoyancy due to entrainment of much moister air. We argue that PCV might play an important role in the transition and cumulus parameterizations could therefore benefit from including them.

Plain Language Summary Cumulonimbus clouds are responsible for many severe weather events and control the water cycle in the atmosphere. Although they are of great importance for both weather forecasting and climate projections, the initiation of these clouds is poorly represented by the numerical models, partially due to our lack of understanding the complex mechanisms controlling the transition from shallow to deep convection. Two possible mechanisms have been proposed to explain the initiation of deep convection: the moistening of the mid–troposphere by the non–precipitating clouds, and the positive feedback of the cold pools induced by the precipitating shallow cumuli. However, recent studies showed that the former is too slow of a process to fully explain the deep initiation, while the later is not able to explain the first phase of the transition. Here, we identify another mechanism, namely the interaction between the passive cloud volumes and the convective updrafts, and argue based on theoretical arguments and numerical experiments why it might play an important role in the rapid transition from shallow to deep convection.

1. Introduction

Despite persistent effort in understanding the complex physical mechanisms controlling the initiation of deep convection in recent years (e.g., Kurowski et al., 2018; Morrison et al., 2022; Peters et al., 2022; Rochetin et al., 2014; Schiro & Neelin, 2019; Wu et al., 2009), numerical weather and climate models are still unable to correctly represent the transition from shallow to deep convection within a diurnal cycle over land (e.g., Bechtold et al., 2004; Chen et al., 2022; Yin & Porporato, 2017), which undermines confidence in climate predictions and the forecasting of severe weather events. Many climate models heavily rely on convective available potential energy (CAPE) and convective inhibition (CIN) conditions to predict the time of storm initiation. This timing has been shown to be shifted by often 2–5 hr earlier when compared with observations or high-resolution simulations (e.g., Christopoulos & Schneider, 2021; Grabowski et al., 2006). Indeed, large CAPE and very small CIN are important requirements for the initiation of deep convection. However, even where these conditions are met, the shallow to deep convection transition may still take several hours or may not even occur at all in a given diurnal cycle (e.g., M. Khairoutdinov & Randall, 2006; Nelson et al., 2021; Tian et al., 2021).

Apart from the conditions on CAPE and CIN, several studies have shown that mid-troposphere relative humidity is an important indicator for the initiation of deep convection (e.g., Sherwood & Wahrlich, 1999; Zhang & Klein, 2010)—a finding that later led to the idea of moisture preconditioning by shallow cumuli controlling the

transition from shallow to deep convection (e.g., Holloway & Neelin, 2009; Waite & Khouider, 2010). In addition to the moistening of the mid-troposphere, shallow cumuli also have a cooling effect on their environment, leading to an increase in CAPE (Yano & Plant, 2012). However, based on observational analysis in the tropics, Hohenegger and Stevens (2013) showed that the transition from shallow to deep convection is too fast to be explained by the shallow preconditioning.

Another possible mechanism that may explain, at least in part, the transition from shallow to deep convection is the organization of the convective field in the boundary layer by cold pools resulting from the first precipitating cumuli (e.g., M. Khairoutdinov & Randall, 2006; Kurowski et al., 2018). As a result, several cumulus parameterization schemes that incorporate cold pool effects have been developed (e.g., Hohenegger & Bretherton, 2011; Rio et al., 2009; Suselj et al., 2019). In a sensitivity experiment, in which cold pools are turned off, Kurowski et al. (2018) shows that cold pools facilitate the development of subsequent convective clouds due to an observed decrease in the entrainment of environmental air into the convective plumes. This could mean that cold pools organize convection into larger plumes, as also brought forward by Schlemmer and Hohenegger (2014). However, although Kurowski et al. (2018) suggest that the cold pool feedback is important for the development of deep cumulonimbus clouds from cumulus congestus, they also show that the transition from shallow to precipitating congestus is not sensitive to the presence of the cold pools. Thus, the explanation based on cold pool effects fails to explain the first phase of the transition. Within a diurnal cycle over land, the increase in the plume radius has also been attributed to the increase in the boundary layer height, as discussed by Grabowski (2023).

In this work, we aim to bring into the discussion the potential role of passive cloud volumes (PCV) in the transition from shallow to deep convection. The distinction between a PCV and a passive cumulus is that a PCV can be only a part of a cumulus that still has other active parts, whereas a passive cumulus is completely passive—there are no active parts within the cloud. Although PCV have been recognized to protect the updrafts from entertainment (e.g., Moser & Lasher-Trapp, 2017), their role in the shallow–to–deep transition has not been previously discussed. We first show from a theoretical perspective why the interaction between the updraft plumes and the PCV may lead to greater cloud top heights. Second, we discuss why the observed increase in the cloud horizontal scale during the transition could be explained by the interaction between plumes and PCV, and why the organization of PCV may lead to even deeper cumulus clouds. We then perform a large–eddy simulation (LES) for a transition case, and analyze the vertical profiles of interacting and non–interacting updrafts.

2. Interaction Between the Passive Clouds and Active Plumes

In order to appreciate the different mechanisms that may lead to deeper clouds during the transition, we return to a classical "ball-on-the-slope" analogy, used in many meteorological textbooks to explain the concept of atmospheric instability and CAPE. CAPE is hereby treated analogous to the gravitational potential energy of a ball rolling down a hill of decreasing slope. It is common that a non–entraining parcel is considered, which means that once the ball is able to overcome the CIN present, reaching the top of the hill—an analogy for the level of free convection (LFC)—the ball will continue to roll until reaching the equilibrium level (EL) of zero slope.

In Figure 1, we schematically present the three discussed mechanisms that may lead to deepening convection. We first consider the sloped surface to be covered by grass, leading to considerable friction between the ball and the grass—an analogy for entrainment. As a result, the ball will be unable to reach the EL, meaning that less potential energy is converted and convection remains shallow (Figure 1a). To motivate the effect of an increase in plume radius consider a larger ball (Figure 1b), which is able to roll further down the hill due to the relatively reduced friction caused by the grass. The analogy can be taken further (Figure 1c), where shallow cumulus preconditioning, which may lead to increased moisture in the cloud layer, is mimicked by a ball that is able to roll further down the hill because the grass is shorter. We also consider that once a ball falls, it bends the grass. The bent grass is an analogy we consider for the passive clouds. Therefore, if a new ball is falling through the exact same place where the grass is already bent, then the ball will experience less friction with the grass, and thus, the ball will again be able to fall deeper (Figure 1d). Throughout this section, only for the purpose of ease of illustration, we simplify the PCV as passive cumuli. However, we do not disregard by any means a situation in which a new updraft interacts with a PCV that is part of a cloud that still has an active part near the top, as in Moser and Lasher-Trapp (2017).

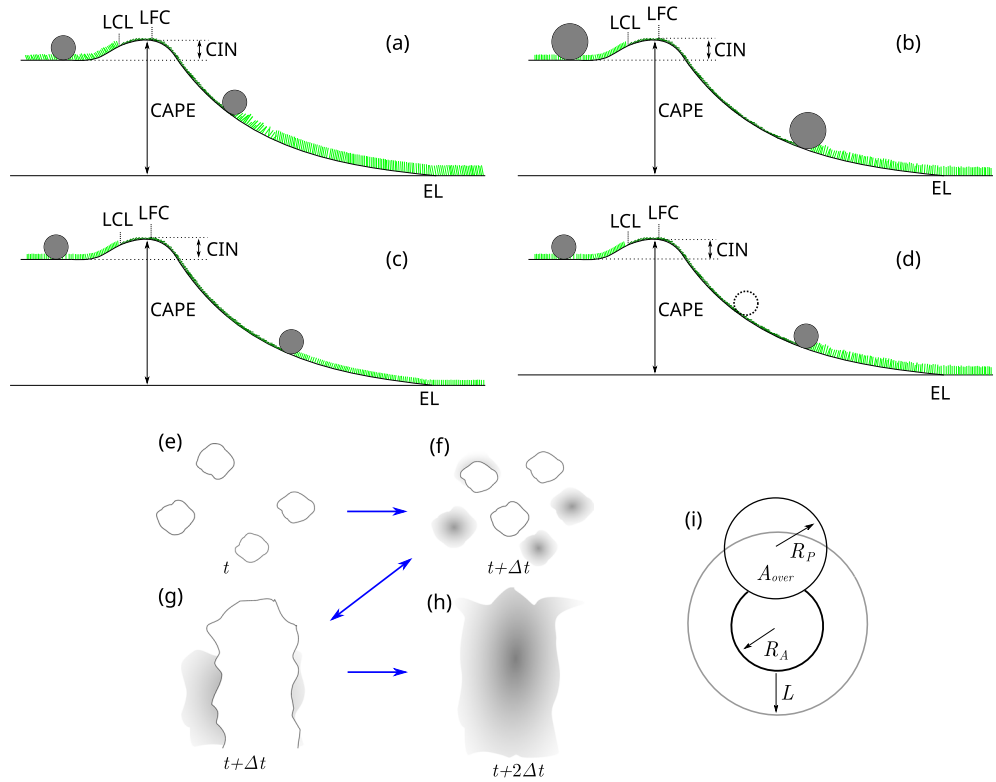

Figure 1. Analogy for deepening convection. A ball rolling down a slope as an analogy for an entraining plume developing in an unstable atmosphere characterized by convective available potential energy (a–d). Friction between the ball and the grass on the slope is an analogy for entrainment. A ball bends the grass as it rolls as an analogy for passive cumuli, illustrated by bent grass of darker color. (a) The ball is stopped due to the friction; (b) a larger ball experiencing less friction; (c) a ball rolling down a greater slope with smaller grass, an analogy for shallow preconditioning; (d) a ball rolling where the grass is bent by a former ball (illustrated by the dotted contour). The interaction between the passive clouds and active plumes (e–i). (e) Top view of an initial cloud field at time t where only active clouds exist; (f) the cloud field at time $t + \Delta t$ at which the initially active clouds become passive (illustrated by the gray color), and other active clouds (plumes) develop; (g) lateral view at the same time as in (f) illustrating the interaction between a passive cumulus cloud and an active plume, leading to a deeper cloud at the time $t + 2\Delta t$, as illustrated in (h). (i) Schematics for the interaction between a passive cloud with a radius R_P and an active plume with a radius R_A, in which the active plume entrains air within an effective distance L.

To understand why the interaction between a plume and a passive cumulus cloud is beneficial for the former, let us consider the Morrison (2017) entraining plume model. In this simple entraining model, the buoyancy B of an entraining parcel can be expressed as:

$$\frac{dB}{dz} = -N^2 - \varepsilon B - \varepsilon \frac{g L_v q_{sE}(1 - RH_E)}{c_p T_E \Gamma}, \tag{1}$$

where z is the vertical coordinate, N^2 is the squared buoyancy frequency, ε is the entrainment rate, g is the gravitational acceleration, L_v is the latent heat of vapourization, q_{sE} is the saturation mixing ratio of the environment, RH_E is the environmental relative humidity, T_E is the temperature of the environment, c_p is the specific heat of air at constant pressure, and $\Gamma \approx 1 + L_v^2 q_{sE} / \left(c_p R_v T_E^2\right)$ is a parameter, for which R_v is the water vapor gas constant. The cumulus parameterization models consider that the plume entrains environmental air with an environment defined at the infinity, not in the direct vicinity of the cloud, neglecting in this way any heterogeneity in the cloud environment. The passive cumulus cloud volumes may represent such a heterogeneity.

If a new plume hits a passive cloud, then this plume will mix with the air of the passive cumulus cloud. Since the passive cloud has no buoyancy, its virtual potential temperature is equal to the environmental virtual potential temperature, and thus it may seem that it is not necessarily beneficial for the plume to entrain the air of the passive cloud. However, if a plume mixes in drier air, this will make some of the liquid water in the active cloud re-evaporate. This re–evaporation process will cool the cloudy air, leading to a decrease in buoyancy.

The contribution of this re–evaporation effect is captured by the last term in Equation 1. In contrast, for a new active plume which entrains the moist air of a passive cloud, the cooling associated with evaporation is reduced, leading to a better preserved buoyancy, and thus, to a higher cloud top. This process is schematically illustrated in Figures 1e–1h. At the onset of shallow convection only active cumuli exist (Figure 1e), whereas at a later time the initial clouds become passive, and new plumes reach the condensation level forming new active clouds (Figure 1f). We consider that there is a finite probability for a new plume to interact with an old passive cloud, leading to a deeper cloud (Figures 1g and 1h).

Thus, Equation 1 should be modified in order to account for the relative humidity of the passive cloud if a new active plume entrains moist air from passive clouds. We consider that the active plume entrains air over a distance given by the mixing length L. Thus, the horizontal area A_{entr} over which the plume entrains environmental air is given by:

$$A_{entr} = \pi\left[(R_A + L)^2 - R_A^2\right] = \pi\left(L^2 + 2R_A L\right). \tag{2}$$

We can therefore modify Equation 1 by replacing RH_E with the relative humidity of entraining air RH_{entr}, given by:

$$RH_{entr} = 100\% \times f + (1 - f)RH_E, \tag{3}$$

for which $f = A_{over}/A_{entr}$ is the fraction of A_{entr} that is occupied by a passive cloud (Figure 1i), for which A_{over} is the area of the overlap.

Here, only to show from a theoretical point of view the contribution of the passive cumuli in the development of the active cumulus clouds, we will consider that $L = 120$ m, as suggested by Morrison (2017). Another obvious alternative will be to consider that L is proportional with the radius of the entraining active plume R_A. We mention here a specific value only to quantify the magnitude of the interaction in the deepening of cumulus clouds, and it should be noted that the specific choice of L is not important for the qualitative theoretical reasoning of this study.

2.1. Idealized Numerical Analysis

We perform a numerical integration of Equation 1 with and without interaction for an idealized vertical profile characterized by a squared buoyancy frequency N^2 of $-1.2 \cdot 10^{-4}$ s^{-2} between the cloud base and 2 km above the cloud base, 10^{-5} s^{-2} between 2 and 10 km above the cloud base, and $2 \cdot 10^{-4}$ s^{-2} between 10 and 11 km above the cloud base (black dotted line in Figure 2), corresponding to a CAPE of 1920 J kg^{-1}. This profile should be taken as a simple, qualitative choice to illustrate the procedure. For the environmental relative humidity, we consider the analytical profile from Weisman and Klemp (1982), and for T_E in Equation 1 we consider a constant value of 300 K for simplicity. We performed a sensitivity test with $T_E = 200$ K, showing no significant difference. For the updraft vertical velocity w_u we consider again the entraining plume model as (de Roode et al., 2012):

$$\frac{dw_u^2}{dz} = 2B - \varepsilon w_u^2. \tag{4}$$

In Equations 1 and 4, for the entrainment rate we consider the following closure: $\varepsilon = \alpha/R_A$, in which $\alpha = 0.2$ is the entrainment coefficient. We thus simulate an interaction between a plume and a passive cloud, in which we consider that the top height of the passive cloud is equal to the top height of the non-interacting cloud, which in turn is given by the height at which $w_u = 0$, and the radius of the passive cloud equals that of the active plume ($R_P = R_A$). We consider these choices for the passive cloud as we are interested here in the situation in which a passive cumulus represented a non–interacting cumulus in the decaying stage. Figure 2 respectively represents the cases without interaction and with perfect interaction. By a perfect interaction we understand that the fraction f is maximum, which means that $A_{over} = \pi R_P^2$. Please note that even for a perfect interaction f is still less than unity. As can be seen in Figure 2, the interaction indeed leads to better preserved positive buoyancy, and as a result, to larger updraft velocities and higher cloud tops. Our simulation suggests that a perfect interaction for a plume with a radius of 300 m is equivalent with an increase of the plume radius to 500 m for the non–interacting case, while an interaction for a plume with a radius of 500 m leads to a higher cloud top than a non–interacting plume with a radius of 700 m. Therefore, our simulation based on the Morrison (2017) plume model suggests that the interaction between passive and active clouds might be at least as important as the increase in updraft radii. However, even with perfect interaction, the clouds might not reach very high altitudes, and as a result will

10.1029/2023GL105996

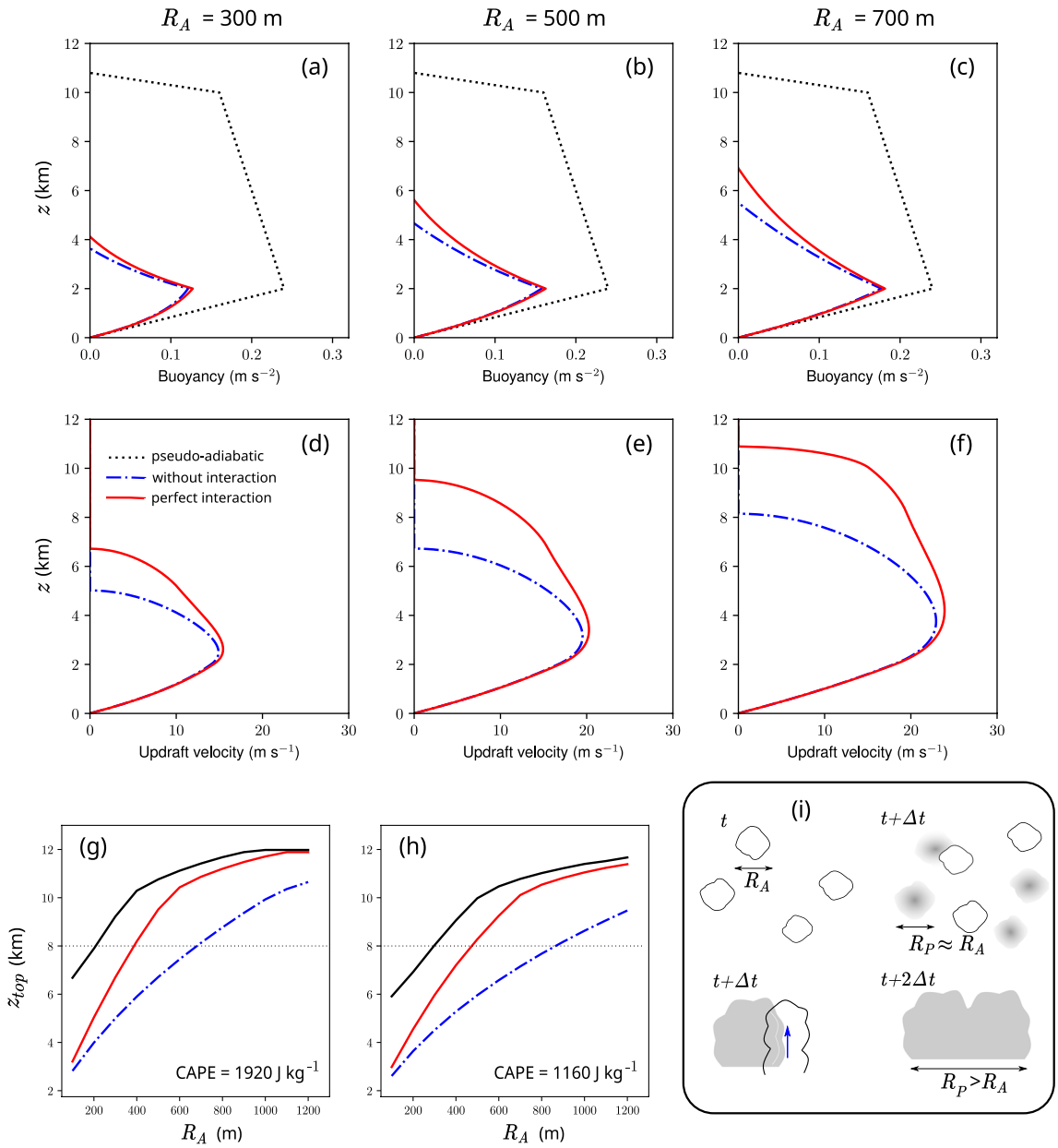

Figure 2. Interaction effect in the conceptual model. Graphical representation of the buoyancy (a–c) and vertical velocity (d–f) for the non–interacting and interacting plumes, respectively. Three values for R_A are considered: 300 m (a, d); 500 m (b, e); 700 m (c, f). (g) Graphical representation of the cloud top for non–interacting (blue dot–dashed line) and interacting for a convective available potential energy (CAPE) of 1920 J kg^{-1}. (h) As in (g) but for a CAPE of 1160 J kg^{-1}. Red solid curves represent a perfect interaction for the case where $R_P = R_A$, and black solid curves represent the case in which $f = 1$. (i) A schematics for the interaction between the passive clouds and the active plumes (as in Figures 1e–1h), leading to larger passive cumuli.

continue to remain shallow. This is because the radius of the passive clouds might be too small to sustain the development of deeper cumuli.

2.2. The Organization of Passive Clouds

If a passive cumulus cloud represents a non–interacting cumulus in the decaying stage, then we expect that the passive cumuli to have spatial scales comparable with those of the active cumuli. Thus, it follows from Equation 3 that RH_{entr} might be too small to help the new plume reach a higher altitude and become deep enough to form a congestus or a cumulonimbus cloud and to trigger positive feedbacks resulting from cold pools. However, if

this is the case, and the interaction only leads to a non-precipitating shallow cumulus cloud, then the interaction might also lead to a passive cloud with a larger radius at a later time, as schematically presented in Figure 2i. Savre and Craig (2023) analyzed the clouds horizontal dimensions for the Large–scale Biosphere–Atmosphere (LBA) transition case (Grabowski et al., 2006), showing that, indeed, the radii of the clouds—identified based on a threshold for the condensed water path—does increase by nearly an order of magnitude during the transition, while the radii of the active plumes—clouds identified based on the updraft criteria—only show a slight increase (see Figure 2 of their study). The increase of the cloud horizontal dimension could be attributed to a process of merging between the clouds. This merging can be of two types: between the active plumes, or between an active plume and a passive cloud. The former leads to an active plume with a larger radius, while the later leads to a larger passive cloud (as schematically presented in Figure 2i).

If a plume interacts with a passive cumulus cloud which has a radius large enough such that A_{over} can become equal with A_{entr}, then $f = 1$ and $RH_{entr} = 100\%$ until the top of the passive cloud is reached. The simulated cloud top height z_{top} for this situation is represented in Figure 2g, together with the case discussed above and the non-interacting case. In Figure 2g we plot the top height of the plumes for the three cases as a function of plume radius. We also present the solutions for a case with a smaller CAPE of 1160 J kg^{-1} (Figure 2h). For this case we considered the same idealized profiles but with $N^2 = -0.8 \cdot 10^{-4}$ s^{-2} between the cloud base and 2 km above the cloud base. As can be seen in Figures 2g and 2h, interaction with a large passive cloud can lead to deep convection even for the very small plumes, whereas the increase in CAPE does not seems to be very important. Note that while the red curve in Figure 2 depends on the choice of mixing length L, the black line is not dependent on this choice, but this situation is conditioned by the increase in the passive clouds dimensions, which has been shown to occur during the transition (Savre & Craig, 2023).

3. Large–Eddy Simulation

Until this point, we showed a model for the interaction of PCV and the new plumes originating from the boundary layer. According to the model, this interaction could lead to larger and deeper clouds and might thus be an important mechanism in the transition from shallow to deep convection. However, one may ask if this process actually occurs during the transition or if the observed rapid organization and deepening of the clouds could be attributed to other unidentified processes. This section is dedicated to this question. To give a preliminary answer, we perform a large-eddy simulation using the System for Atmospheric Modeling (SAM), version 6.11 (M. F. Khairoutdinov & Randall, 2003) for the LBA transition case with the sounding for temperature and relative humidity as in Grabowski et al. (2006). Here, we consider an imposed diurnal cycle for the surface temperature $T_s(t)$ given by $T_s(t) = 300\text{ K} + 12\text{ K} \cdot \sin(2\pi t/24\text{ hr})$, in which t is the simulated time, resulting in maximum surface latent and sensible heat fluxes of approximately 240 W m^{-2} and 35 W m^{-2}, respectively. The square domain is doubly periodic in the horizontal directions, with 51.2 km linear domain dimension, with a horizontal grid length of 50 m, and a vertical grid length of 50 m near the surface that gradually coarsens to 500 m near the domain top at 26 km, with 100 vertical levels used in total. As the presence of mean horizontal flow might also play a role in the transition (Grabowski, 2023), the horizontal wind field is initially set to zero everywhere. In our case, CAPE increases from around 1450 J kg^{-1} at the start of the simulation to 2600 J kg^{-1} after 10 hr, at the end of the simulation.

We analyze the 3D model output every 4 minutes in order to classify every grid cell as an interacting, non–interacting or passive cloud cell. We consider that a cloud grid cell is one in which the total water condensate lies above a threshold of 10^{-3} g kg^{-1}, and a cloudy updraft is present in a cloud cell where the vertical velocity is above 0.1 m s^{-1}. If the cloud cell is not also an updraft cell, we consider it to be a passive cloud cell. We further label each cloudy updraft as an interacting or non-interacting updraft: If at a given time a cell is a cloudy updraft but at a previous time (4 minutes earlier) the cell was a passive cloud cell, then we consider the cell to be an interacting cell. Because an updraft entrains air from its vicinity, we also consider that a cell is interacting if any of its horizontal neighbors were passive cloud cells at the previous time, but only if the cell was not an updraft at the previous time (to avoid counting as interacting the cloudy cells close to the subsidizing shells of the clouds). In addition, we consider that if an updraft was labeled as interacting at the previous time step, then it is still interacting. Since an interacting plume may overshoot the top of the passive cloud, we consider that if at a vertical level k the updraft is interacting, and at the level $k + 1$ there is a cloudy updraft, then this updraft is also interacting. Note that this classification is unable to account for the interacting plumes that are already detached

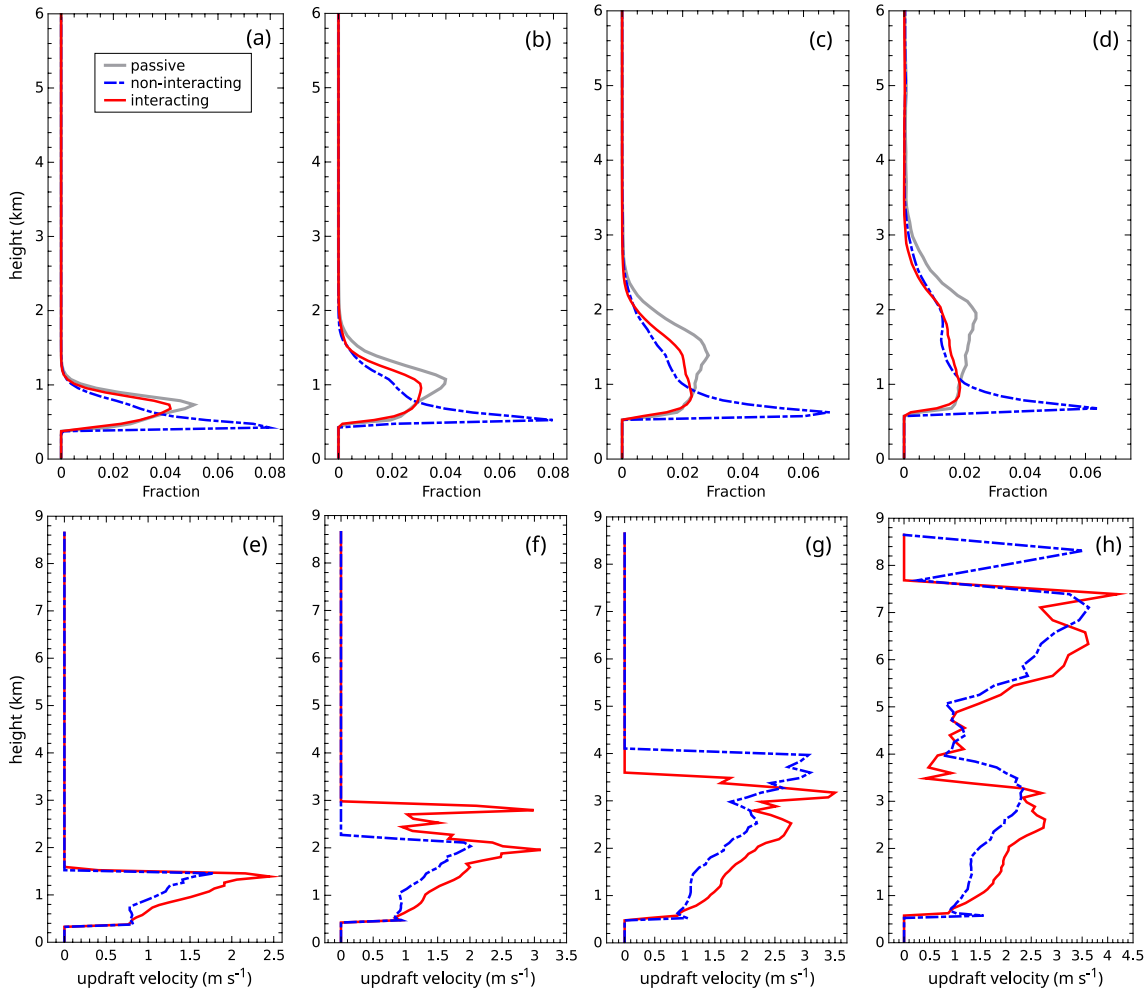

Figure 3. Interaction effect in large-eddy simulations. Graphical representation of the fraction (a–d) and mean updraft velocity (e–f) of passive (gray solid line), updraft non–interacting (blue dot–dashed line), and updraft interacting (red solid line) cloudy cells as a function of height at the following times: 4 hr (a, e), 5 hr (b, f), 6 hr (c, g), and 7 hr (d, h).

from the passive cloud, for example, a bubble or the tail of a plume that is already above the top of the passive cloud. Thus, at the cloud tops, the number of interacting cells might be underestimated. However, our scope here is to show whether or not the interaction between the passive clouds and the updrafts plumes does occur during the transition, and whether or not the vertical velocity of the interacting updrafts is larger than the vertical velocity of the non–interacting updrafts.

In Figures 3a–3d we present the vertical profiles for the fractional areas occupied by the passive, interacting, and non–interacting cloudy cells, at every height, during the transition. It is seen that the fraction of interacting updrafts do not decrease with height as rapidly as the non–interacting one, suggesting that the interacting updrafts preserve their buoyancy better then the non–interacting ones. However, at the cloud tops, the updrafts are not necessarily only interacting, suggesting that although the interaction is important for the fate of the rising plumes, it does not necessarily lead to higher cloud tops over the whole domain. However, as mentioned above, the fraction of interacting updrafts at the top might be underestimated by our methodology. In any case, immediately above cloud base, the fraction of interacting updrafts becomes larger then the fraction of non-interacting updrafts (Figures 3a–3d), suggesting that the boundary layer plumes reach the LFC much more easily in locations where PCV are already present. Thus, we show that the PCV have also an important role in helping the plumes reach the LFC. As a result, more and more humidity is transported by the plumes from the boundary layer in a very small fraction of the cloud environment, which may be seen as a type of shallow local preconditioning. Moreover, as predicted, the updraft velocity of the interacting cells is larger then the updraft velocity of non–interacting

cells, at least close to the cloud base (Figures 3e–3h). However, at hour 6 and 7 it seems that close to the cloud top, although the fraction of updraft cells is very small, the non–interacting updraft velocity is larger than the interacting updraft velocity. This might be due to our methodology which underestimates the fraction of interacting cells close to the cloud top, or due to cold pools that organize the convection into larger plumes that are able to rise higher.

4. Discussion and Conclusion

This study aimed to pinpoint the potential impact of heterogeneity in the cloud environment, due to initial shallow cumuli, on the development of subsequent deep convection. Such heterogeneity can result from PCV, which we call areas where air is saturated but not convective. Although here we only discuss the role of PCV and work under rather idealized settings, future studies could analyze the impact of those areas in which the relative humidity is much larger than the average yet below saturation. Moreover, a pair of simulations with piggybacking methodology (e.g., Kurowski et al., 2019) might provide more direct evidence of the role of PCV in the transition.

Our main reasoning here is that the air entrained by active cumulus clouds is not well-characterized by average values over a large domain, as considered by the cumulus parameterization models. Rather, cumuli entrain air from their immediate vicinity, and this air is not necessarily well-represented by a domain mean value. This aspect might be very important for the transition from shallow-to-deep convection, especially if the number of updrafts that develop where the PCV are already present cannot be neglected during the transition. Our findings suggest that more than half of the convective updrafts interact with old PCV immediately above the cloud base, which may show that the PCV help the updrafts to reach the LFC. Using an entraining plume model, we show why, theoretically, this interaction is beneficial for the development of deeper clouds. We argue that the observed increase in the cloud horizontal dimensions could also be attributed to the interaction between the PCV and the new plumes originating from the boundary layer, and show why this organization leads to even deeper clouds.

Due to the relatively small domain size and short duration of the simulation we focused here on local–scale convective organization. It would be an interesting extension to study larger domain sizes and timescales, especially multi–day diurnal cycles, where mesoscale convective organization is known to self–organize the moisture field (Jensen et al., 2022) and thus precondition the transition to deep convection we describe.

Data Availability Statement

The LES data from Figure 3 are openly available at Vraciu (2023). The data from Figure 2 are obtained as indicated in the text using the Matplotlib (Caswell et al., 2020) and Numpy (Harris et al., 2020) libraries.

Acknowledgments
The authors thank W. W. Grabowski as well as another anonymous reviewer for insightful comments on the manuscript. The authors gratefully acknowledge funding by a grant from the VILLUM Foundation (Grant 13168) and the European Research Council (ERC) under the European Union's Horizon 2020 research and innovation program (Grant 771859) and the Novo Nordisk Foundation Interdisciplinary Synergy Program (Grant NNF19OC0057374). This work used resources of the Deutsches Klimarechenzentrum (DKRZ), granted by its Scientific Steering Committee (WLA) under project ID bb1166. CVV also acknowledge financial support from the Romanian Ministry of Research, Innovation and Digitization through Project PN 23 21 01 01/2023.

References

Bechtold, P., Chaboureau, J.-P., Beljaars, A., Betts, A., Köhler, M., Miller, M., & Redelsperger, J.-L. (2004). The simulation of the diurnal cycle of convective precipitation over land in a global model. *Quarterly Journal of the Royal Meteorological Society*, *130*(604), 3119–3137. https://doi.org/10.1256/qj.03.103

Caswell, T., Droettboom, M., Lee, A., Hunter, J., Firing, E., Stansby, D., et al. (2020). Matplotlib v3.2.1 [Software]. Zenodo. https://doi.org/10.5281/zenodo.3714460

Chen, G., Wang, W.-C., Bao, Q., & Li, J. (2022). Evaluation of simulated cloud diurnal variation in CMIP6 climate models. *Journal of Geophysical Research: Atmospheres*, *127*(6), e2021JD036422. https://doi.org/10.1029/2021jd036422

Christopoulos, C., & Schneider, T. (2021). Assessing biases and climate implications of the diurnal precipitation cycle in climate models. *Geophysical Research Letters*, *48*(13), e2021GL093017. https://doi.org/10.1029/2021gl093017

de Roode, S. R., Siebesma, A. P., Jonker, H. J., & de Voogd, Y. (2012). Parameterization of the vertical velocity equation for shallow cumulus clouds. *Monthly Weather Review*, *140*(8), 2424–2436. https://doi.org/10.1175/mwr-d-11-00277.1

Grabowski, W. (2023). Daytime convective development over land: The role of surface forcing. *Quarterly Journal of the Royal Meteorological Society*. https://doi.org/10.1002/qj.4532

Grabowski, W., Bechtold, P., Cheng, A., Forbes, R., Halliwell, C., Khairoutdinov, M., et al. (2006). Daytime convective development over land: A model intercomparison based on LBA observations. *Quarterly Journal of the Royal Meteorological Society*, *132*(615), 317–344. https://doi.org/10.1256/qj.04.147

Harris, C. R., Millman, K. J., Van Der Walt, S. J., Gommers, R., Virtanen, P., Cournapeau, D., et al. (2020). Array programming with NumPy [Software]. Nature, *585*(7825), 357–362. https://doi.org/10.1038/s41586-020-2649-2

Hohenegger, C., & Bretherton, C. S. (2011). Simulating deep convection with a shallow convection scheme. *Atmospheric Chemistry and Physics*, *11*(20), 10389–10406. https://doi.org/10.5194/acp-11-10389-2011

Hohenegger, C., & Stevens, B. (2013). Preconditioning deep convection with cumulus congestus. *Journal of the Atmospheric Sciences*, *70*(2), 448–464. https://doi.org/10.1175/jas-d-12-089.1

Holloway, C. E., & Neelin, J. D. (2009). Moisture vertical structure, column water vapor, and tropical deep convection. *Journal of the Atmospheric Sciences*, *66*(6), 1665–1683. https://doi.org/10.1175/2008jas2806.1

Jensen, G. G., Fiévet, R., & Haerter, J. O. (2022). The diurnal path to persistent convective self-aggregation. *Journal of Advances in Modeling Earth Systems*, *14*(5), e2021MS002923. https://doi.org/10.1029/2021ms002923

Khairoutdinov, M., & Randall, D. (2006). High-resolution simulation of shallow-to-deep convection transition over land. *Journal of the Atmospheric Sciences*, *63*(12), 3421–3436. https://doi.org/10.1175/jas3810.1

Khairoutdinov, M. F., & Randall, D. A. (2003). Cloud resolving modeling of the arm summer 1997 iop: Model formulation, results, uncertainties, and sensitivities. *Journal of the Atmospheric Sciences*, *60*(4), 607–625. https://doi.org/10.1175/1520-0469(2003)060<0607:crmota>2.0.co;2

Kurowski, M. J., Suselj, K., & Grabowski, W. W. (2019). Is shallow convection sensitive to environmental heterogeneities? *Geophysical Research Letters*, *46*(3), 1785–1793. https://doi.org/10.1029/2018gl080847

Kurowski, M. J., Suselj, K., Grabowski, W. W., & Teixeira, J. (2018). Shallow-to-deep transition of continental moist convection: Cold pools, surface fluxes, and mesoscale organization. *Journal of the Atmospheric Sciences*, *75*(12), 4071–4090. https://doi.org/10.1175/jas-d-18-0031.1

Morrison, H. (2017). An analytic description of the structure and evolution of growing deep cumulus updrafts. *Journal of the Atmospheric Sciences*, *74*(3), 809–834. https://doi.org/10.1175/jas-d-16-0234.1

Morrison, H., Peters, J. M., Chandrakar, K. K., & Sherwood, S. C. (2022). Influences of environmental relative humidity and horizontal scale of subcloud ascent on deep convective initiation. *Journal of the Atmospheric Sciences*, *79*(2), 337–359. https://doi.org/10.1175/jas-d-21-0056.1

Moser, D. H., & Lasher-Trapp, S. (2017). The influence of successive thermals on entrainment and dilution in a simulated cumulus congestus. *Journal of the Atmospheric Sciences*, *74*(2), 375–392. https://doi.org/10.1175/jas-d-16-0144.1

Nelson, T. C., Marquis, J., Varble, A., & Friedrich, K. (2021). Radiosonde observations of environments supporting deep moist convection initiation during relampago-cacti. *Monthly Weather Review*, *149*(1), 289–309. https://doi.org/10.1175/mwr-d-20-0148.1

Peters, J. M., Morrison, H., Nelson, T. C., Marquis, J. N., Mulholland, J. P., & Nowotarski, C. J. (2022). The influence of shear on deep convection initiation. Part I: Theory. *Journal of the Atmospheric Sciences*, *79*(6), 1669–1690. https://doi.org/10.1175/jas-d-21-0145.1

Rio, C., Hourdin, F., Grandpeix, J.-Y., & Lafore, J.-P. (2009). Shifting the diurnal cycle of parameterized deep convection over land. *Geophysical Research Letters*, *36*(7), L07809. https://doi.org/10.1029/2008gl036779

Rochetin, N., Couvreux, F., Grandpeix, J.-Y., & Rio, C. (2014). Deep convection triggering by boundary layer thermals. Part I: Les analysis and stochastic triggering formulation. *Journal of the Atmospheric Sciences*, *71*(2), 496–514. https://doi.org/10.1175/jas-d-12-0336.1

Savre, J., & Craig, G. (2023). Fitting Cumulus cloud size distributions from idealized cloud resolving model simulations. *Journal of Advances in Modeling Earth Systems*, *15*(5), e2022MS003360. https://doi.org/10.1029/2022ms003360

Schiro, K. A., & Neelin, J. D. (2019). Deep convective organization, moisture vertical structure, and convective transition using deep-inflow mixing. *Journal of the Atmospheric Sciences*, *76*(4), 965–987. https://doi.org/10.1175/jas-d-18-0122.1

Schlemmer, L., & Hohenegger, C. (2014). The formation of wider and deeper clouds as a result of cold-pool dynamics. *Journal of the Atmospheric Sciences*, *71*(8), 2842–2858. https://doi.org/10.1175/jas-d-13-0170.1

Sherwood, S. C., & Wahrlich, R. (1999). Observed evolution of tropical deep convective events and their environment. *Monthly Weather Review*, *127*(8), 1777–1795. https://doi.org/10.1175/1520-0493(1999)127<1777:oeotdc>2.0.co;2

Suselj, K., Kurowski, M. J., & Teixeira, J. (2019). A unified eddy-diffusivity/mass-flux approach for modeling atmospheric convection. *Journal of the Atmospheric Sciences*, *76*(8), 2505–2537. https://doi.org/10.1175/jas-d-18-0239.1

Tian, Y., Zhang, Y., Klein, S. A., & Schumacher, C. (2021). Interpreting the diurnal cycle of clouds and precipitation in the arm goamazon observations: Shallow to deep convection transition. *Journal of Geophysical Research: Atmospheres*, *126*(5), e2020JD033766. https://doi.org/10.1029/2020jd033766

Vraciu, C. V. (2023). LES data presented in "The role of passive cloud volumes in the transition from shallow to deep atmospheric convection" [Dataset]. Zenodo. https://doi.org/10.5281/zenodo.8275881

Waite, M. L., & Khouider, B. (2010). The deepening of tropical convection by congestus preconditioning. *Journal of the Atmospheric Sciences*, *67*(8), 2601–2615. https://doi.org/10.1175/2010jas3357.1

Weisman, M. L., & Klemp, J. B. (1982). The dependence of numerically simulated convective storms on vertical wind shear and buoyancy. *Monthly Weather Review*, *110*(6), 504–520. https://doi.org/10.1175/1520-0493(1982)110<0504:tdonsc>2.0.co;2

Wu, C.-M., Stevens, B., & Arakawa, A. (2009). What controls the transition from shallow to deep convection? *Journal of the Atmospheric Sciences*, *66*(6), 1793–1806. https://doi.org/10.1175/2008jas2945.1

Yano, J.-I., & Plant, R. (2012). Interactions between shallow and deep convection under a finite departure from convective quasi equilibrium. *Journal of the Atmospheric Sciences*, *69*(12), 3463–3470. https://doi.org/10.1175/jas-d-12-0108.1

Yin, J., & Porporato, A. (2017). Diurnal cloud cycle biases in climate models. *Nature Communications*, *8*(1), 2269. https://doi.org/10.1038/s41467-017-02369-4

Zhang, Y., & Klein, S. A. (2010). Mechanisms affecting the transition from shallow to deep convection over land: Inferences from observations of the diurnal cycle collected at the arm southern Great Plains site. *Journal of the Atmospheric Sciences*, *67*(9), 2943–2959. https://doi.org/10.1175/2010jas3366.1